Electronic Supplementary Material (ESI) for Inorganic Chemistry Frontiers.

Electronic Supporting Information

Boosting photoelectrochemical water splitting of Fe_2O_3 by surface states regulation

Shanshan Jiang[a], Xinxin Zhang[a], Madiha Nawaz[a], Xiaoxing Fan[a, b*] , Ran Tao[a, b#]

[a] School of Physics, Liaoning University, Shenyang, 110036. P. R. China.

[b] Liaoning Key Laboratory of Semiconductor Light Emitting and Photocatalytic Materials, Liaoning University, Shenyang 110036, P. R. China.

*Corresponding author. E-mail address: xxfan@lnu.edu.cn

Corresponding author. E-mail address: taoran@lnu.edu.cn

Contents of Supplementary

1. Experimental section

1.1 Characterization

The crystal structure of Fe_2O_3-based photoanode was characterized using X-ray diffraction (XRD, TD-3500). The morphology and cross-section of the thin films were observed using a scanning electron microscope (FE-SEM, Regulus 8100), and the elements present in the film were further tested using energy dispersive X-ray spectroscopy (EDS, Oxford). X-ray photoelectron spectroscopy (XPS, UIVAC-PHI) measurements of the photoanode film's elemental composition and chemical state were conducted using a PHI 5000 Verse probe. The UV-visible diffuse reflectance spectroscopy (UV-vis DRS) was measured at room temperature using a UV-2600 spectrophotometer (Shimadzu, Japan).

1.2 PEC performance test

The PEC performance was measured on an electrochemical workstation (Princeton Applied Research 2273 model) using a standard three-electrode system. The light intensity was set to 100 mW/cm^2, equivalent to 1 Sun at AM 1.5G. The standard three-electrode system consisted of Pt as the counter electrode, Ag/AgCl as the reference electrode, and Fe_2O_3-based photoelectrodes as the working electrode. The PEC performance was measured in the 1 M NaOH (pH≈13.6) electrolyte. Electrochemical impedance spectroscopy (EIS) measurements was conducted with the frequency ranging from 10 kHz to 0.1 Hz. Gas evolution was analyzed by gas chromatography (GC1690, JieDao) with a three-electrode system.

2. The equations

Eq S1 was used to convert Ag/AgCl reference potential into **RHE**[1]:

$$V_{RHE} = V_{Ag/Agcl} + 0.197 + 0.059\,pH \quad \text{S1}$$

Eq S2 was used to calculate **IPCE**[2]:

$$IPCE = \frac{J \times 1240}{\lambda \times P_{light}} \times 100\% \quad \text{S2}$$

Where J is the photocurrent density (mA/cm^2); λ is the incident light wavelength (nm); P_{light} is the power density (mW/cm^2).

Eq S3 was used to calculate **ABPE**[3]:

$$ABPE = \frac{J(1.23 - V_b)}{P} \times 100\% \quad \text{S3}$$

where J is the photocurrent density of samples, V_b is the applied external potential *vs.* RHE and P_{light} is the power density of the illumination (100 mWcm^{-2}).

Eq S4 was used to calculate **The Faraday efficiencies**[4]:

$$H_2(or\ O_2)\mu mol.cm^{-2} = \left(\frac{Area\ of\ H_2(or\ O_2)peak}{Slope\ of\ calibration\ curve\ for\ H_2(or\ O_2)}\right) \times (Head\ space\ volume) \times \left(\frac{1mol}{24.2\ L}\right) \quad \text{S4}$$

Faradic efficiency=Actual photocurrent density/Theoretical photocurrent density

Actual photocurrent density = N× nH_2/O_2 × F S5

Where F is the Faraday constant which is 0.096487 C/μmol. nH_2/O_2 (μmol) is amount of H_2 or O_2 evolution determined by gas chromatography. N is number of electrons needed to evolve one molecule of H_2 or O_2. It is assumed that 2 electrons are needed to produce one molecule of H_2, and 4 electrons are needed for one molecule of O_2.

Eq S6 was used to calculate **LHE**[5]**:**

$$LHE = 1-10^{-A(\lambda)} \quad \text{S6}$$

where $A_{(\lambda)}$ is absorbance, λ is wavelength.

Eq S7 was used to calculate $\mathbf{J_{abs}}$[6]**:**

$$J_{abs} = \frac{q}{hc}\int_{\lambda}^{\lambda_2} \lambda \phi_{\lambda} \eta_{abs} d\lambda \quad \text{S7}$$

Where h was the Plank constant, c was the light speed, $\phi_{\lambda}$was the photon flux of the AM 1.5G solar spectrum, and η_{abs} was the light absorption efficiency.

Eq S8 was used to calculate η_{sep}[7]**:**

$$\eta_{sep} = \frac{J_{Na_2SO_3}}{J_{abs}} \quad \text{S8}$$

Where The $J_{Na_2SO_3}$ was the photocurrent density measured in 1 M KOH and 0.5 M Na_2SO_3 mixed electrolyte, which served as hole scavengers to ensure the hole injection rate approaching 100%.

Eq S9 was used to calculate η_{inj}[8]**:**

$$\eta_{inj} = \frac{J_{H_2O}}{J_{Na_2SO_3}} \quad \text{S9}$$

Where J_{H_2O} was the photocurrent densities measured in 1 M KOH.

Eq S10 was used to calculate $\mathbf{N_D}$[9]**:**

$$\frac{1}{C^2} = \left(\frac{2}{e\varepsilon\varepsilon_0 N_D A^2}\right)\left(V - V_{fb} - \frac{k_B T}{q}\right) \quad \text{S10}$$

Where C was the space-charge capacitance, V (V vs. RHE) was the applied voltage, V_{fb} (V vs. RHE) was the flat-band potential, N_D was the charge carrier density, ε was

the dielectric constant of the semiconductor (80 for α-Fe_2O_3). ε_0 was the vacuum permittivity (8.854 x 10^{-12} F/m), k_B was the Boltzmann constant(1.38×10^{-23} J K^{-1}), q was the electronic charge (1.60 x10^{-19} C), and T was the absolute temperature (298K).

Eq S11 was used to calculate τ_e[10]:

$$\tau_e = \frac{1}{2\pi f_{max}} \quad \text{S11}$$

Where f_{max} is the frequency when phase reaches peak.

Eq S12 was used to calculate C_{dl}[11]:

$$ECSA \propto C_{dl} = \frac{dQ/dt}{dV/dt} = \frac{j(V)}{v} \quad \text{S12}$$

Where C_{dl} indicates the double-layer electrochemical capacitance, j(V) is the capacitive current measured at potential V, and v is the scan rate.

Eq S13 was used to calculate **DOS**[12]:

$$N_{SS}(E) = \frac{C_{trap}(E)}{q} \quad \text{S13}$$

Where Nss (E) is the DOS ($cm^{-2}\cdot eV^{-1}$) as a function of the applied potential and q is the electron charge (1.602 × 10−19 C).

Eq S13 was used to calculate **the proportion of charge transferred** at the photoanode/electrolyte interface[13]:

$$Transfer\ efficiency(\%) = \frac{K_{ct}}{K_{ct} + K_{trapping}} = \frac{R_{trapping}}{R_{ct} + R_{trapping}}$$

S14

Where K_{ct} and $K_{trapping}$ are the charge transfer and trapping rate constants, respectively, and R_{ct} and $R_{trapping}$ are the corresponding resistances.

3. Supplementary Figures

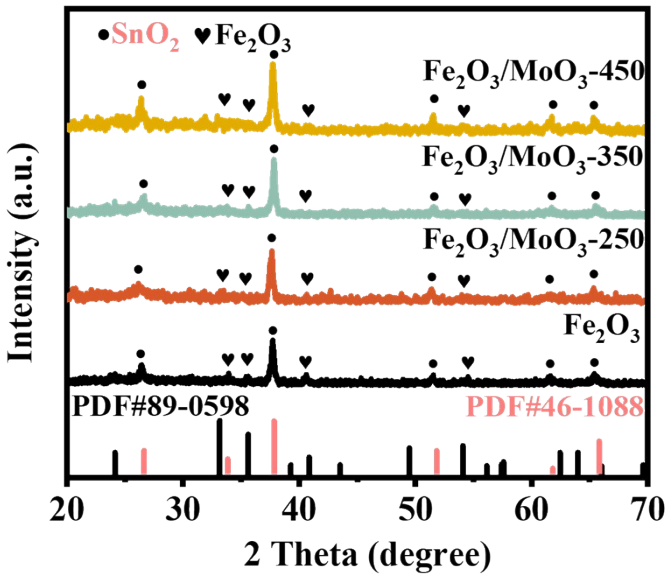

Fig. S1. XRD pattern of Fe_2O_3, Fe_2O_3/MoO_3-250, Fe_2O_3/MoO_3-350 and Fe_2O_3/MoO_3-450 films

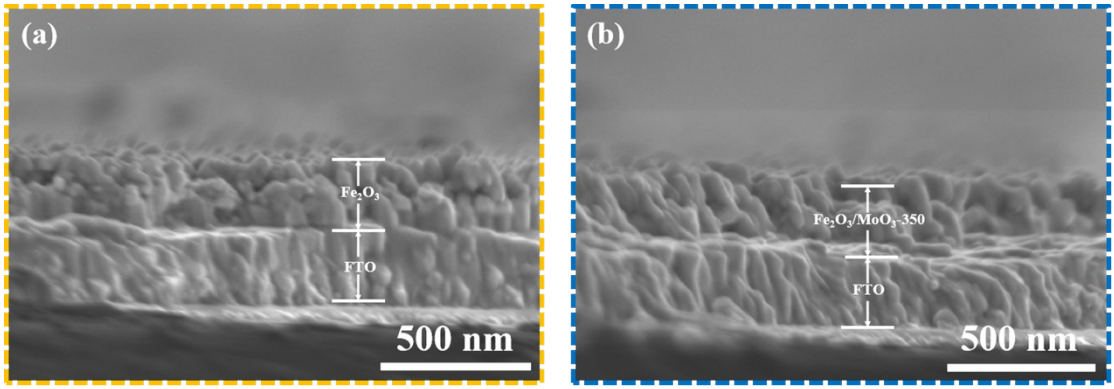

Fig. S2. The cross section images of $Fe_2O_3$and Fe_2O_3/MoO_3-350 films.

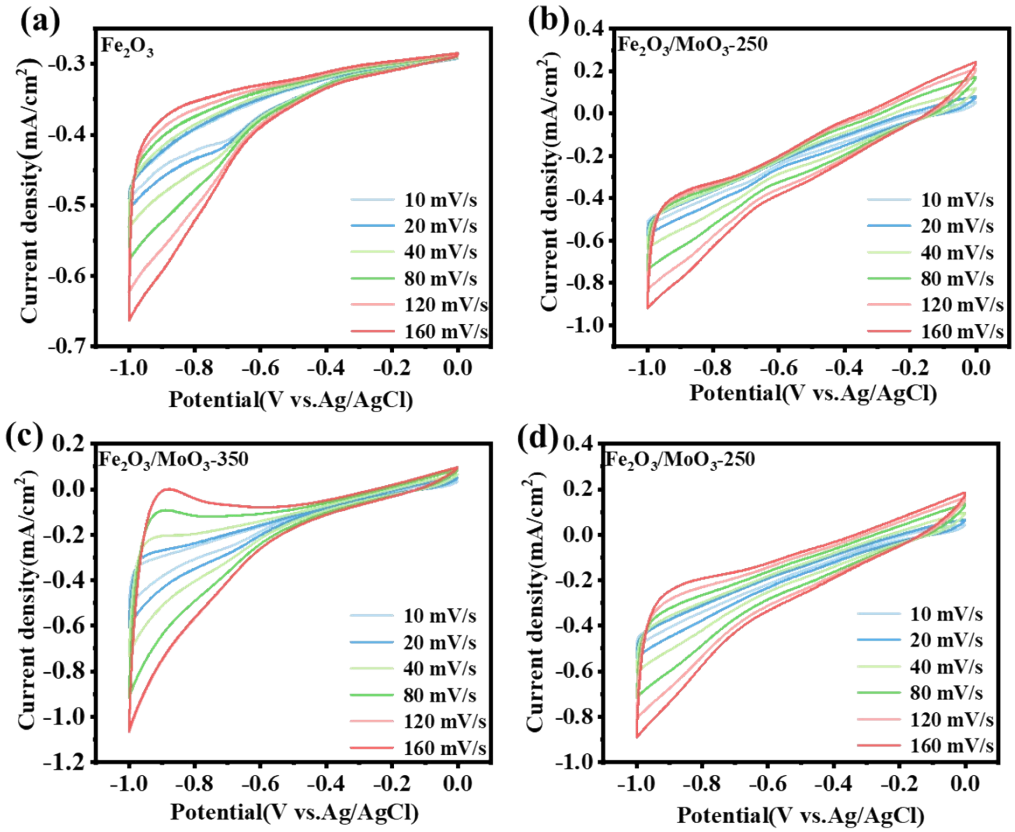

Fig. S3. ECSA of Fe_2O_3, Fe_2O_3/MoO_3-250, Fe_2O_3/MoO_3-350 and Fe_2O_3/MoO_3-450 films.

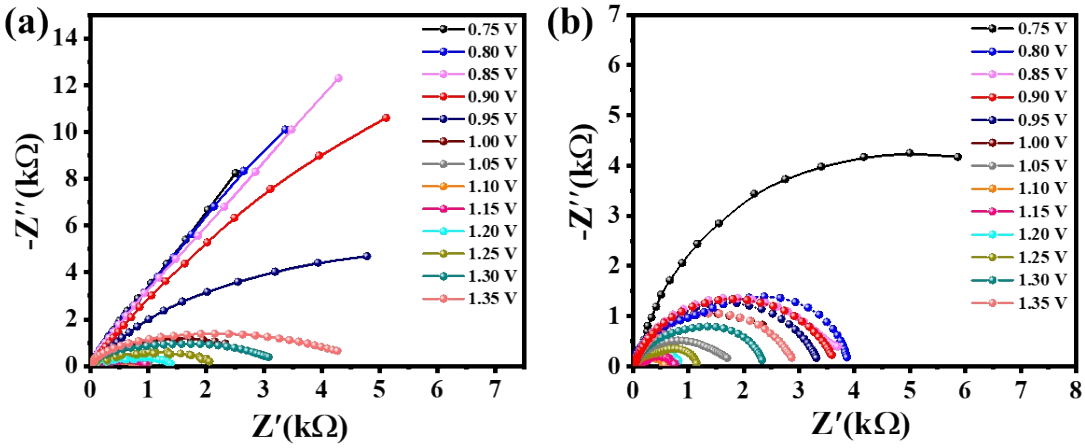

Fig. S4. The PEIS results for (a) Fe_2O_3 and (b) Fe_2O_3/MoO_3-350 photoanodes at different applied biases under constant light illumination (100 mW/cm^2).

Table S1. Fitting results of EIS measurement

Samples	R_s (Ω)	R_{bulk} (Ω)	R_{ct} (Ω)	$\tau_e(ms)$
Fe_2O_3	45.2	109.1	23830	20.1
Fe_2O_3/MoO_3-250	41.7	50.8	1974.5	50.4
Fe_2O_3/MoO_3-350	39.4	33.9	997.2	52.1
Fe_2O_3/MoO_3-450	40.6	73.8	4054.6	31.8

4. References

1 Y. Zhao, M. Duan, C. Deng, J. Yang, S. Yang, Y. Zhang, H. Sheng, Y. Li, C. Chen and J. Zhao, Br^-/BrO^--mediated highly efficient photoelectrochemical epoxidation of alkenes on alpha-Fe_2O_3, *Nat. Commun.*, 2023, **14**, 1943-1952.

2 B. Jin, Y. Lu, X. Zhang, X. Zhang, D. Li, Q. Liu, B. Deng and H. Li, Iceberg-inspired solar water generator for enhanced thermoelectricity–freshwater synergistic production, *Chem. Eng. J.*, 2023, **469**, 143906.

3 J. Zhang, J. Zhang, C. Dong, Y. Xia, L. Jiang, G. Wang, R. Wang and J. Chen, Direct Growth of Polymeric Carbon Nitride Nanosheet Photoanode for Greatly Efficient Photoelectrochemical Water-Splitting, *Small*, 2023, **19**, 2208049.

4 S. Li, S. M. Jung, W. Chung, J. W. Seo, H. Kim, S. I. Park, H. C. Lee, J. S. Han, S. B. Ha, I. Y. Kim, S. I. In, J. Y. Kim and J. Yang, Defect engineering of ternary Cu–In–Se quantum dots for boosting photoelectrochemical hydrogen generation, *Carbon Energy*, 2023, **384**, 1-14.

5 H. M. Chen, C. K. Chen, R. S. Liu, L. Zhang, J. Zhang and D. P. Wilkinson, Nano-architecture and material designs for water splitting photoelectrodes, *Chem. Soc. Rev.*, 2012, **41**, 5654-5671.

6 Y. Wang, Q. Pan, Y. Qiao, X. Wang, D. Deng, F. Zheng, B. Chen and J. Qiu, Layered Metal Oxide Nanosheets with Enhanced Interlayer Space for Electrochemical Deionization, *Adv. Mater.*, 2023, **35**, 2210871.

7 M. G. Lee, J. W. Yang, I. J. Park, T. H. Lee, H. Park, W. S. Cheon, S. A. Lee, H. Lee, S. G. Ji, J. M. Suh, J. Moon, J. Y. Kim and H. W. Jang, Tailored $BiVO_4/In_2O_3$ nanostructures with boosted charge separation ability toward unassisted water splitting, *Carbon Energy*, 2023, **321**, 1-15.

8 K. Wang, H. Ni, W. Zhao, X. Wu, Y. Hu, G. Xiao and F. Jiang, Highly efficient GeSe micro-air-brick-based thin film standalone solar water-splitting photoelectrode with solar-light-soaking accumulation process, *Energy Environ. Sci.*, 2023, **16**, 1155-1165.

9 H.-J. Ahn, K.-Y. Yoon, M. Sung, H. Yoo, H. Ahn, B. H. Lee, J. Lee and J.-H. Jang, Utilizing a Siloxane-Modified Organic Semiconductor for Photoelectrochemical Water Splitting, *ACS Energy Lett.*, 2023, **8**, 2595-2602.

10 L. Wang, J. Zhang, Y. Li, Y. Shi, J. Huang, Q. Mei, L. Wang, F. Ding, B. Bai and Q. Wang, Heterostructured $CoFe_{1.5}Cr_{0.5}S_3O$/COFs/$BiVO_4$ photoanode boosts charge extraction for efficient photoelectrochemical water splitting, *Appl. Catal. B: Environ.*, 2023, **336**, 122921.

11 R. Ghosh, B. Papnai, Y. S. Chen, K. Yadav, R. Sankar, Y. P. Hsieh, M. Hofmann and Y. F. Chen, Heterostructured $CoFe_{1.5}Cr_{0.5}S_3O$/COFs/$BiVO_4$ photoanode boosts charge extraction for efficient photoelectrochemical water splitting, *Adv. Mater.*, 2023, **35**, 2210746.

12 H. Zhang, G. She, J. Xu, S. Li, Y. Liu, J. Luo and W. Shi, Electrochemical and photoelectrochemical water oxidation of solvothermally synthesized Zr-doped α-Fe_2O_3 nanostructures, *J. Mater. Chem.A*, 2022, **10**, 4952-4959.

13. C. Venkata Reddy, I. N. Reddy, B. Akkinepally, K. R. Reddy and J. Shim, Synthesis and photoelectrochemical water oxidation of (Y, Cu) codoped α-Fe_2O_3 nanostructure photoanode, *J. Alloys Compd.*, 2020, **814**, 152349.